DMD Fast Forward. Published on December 18, 2015 as DOI: 10.1124/dmd.115.067439
This article has not been copyedited and formatted. The final version may differ from this version.

Title page

Effects of Phenobarbital on Expression of UDP-glucuronosyltransferase 1a6 and 1a7 in Rat Brain

Yukiko Sakakibara, Miki Katoh, Yuya Kondo, and Masayuki Nadai

Pharmaceutics, Faculty of Pharmacy, Meijo University; 150 Yagotoyama, Tenpaku-ku, Nagoya 468–8503, Japan

DMD Fast Forward. Published on December 18, 2015 as DOI: 10.1124/dmd.115.067439
This article has not been copyedited and formatted. The final version may differ from this version.

Running title page

a) Running title: Phenobarbital alters brain UGT in rats

b) Correspondence author: Miki Katoh, PhD, Pharmaceutics, Faculty of Pharmacy, Meijo University; 150 Yagotoyama, Tenpaku-ku, Nagoya 468–8503, Japan. E-mail: mkatoh@meijo-u.ac.jp, Tel: +81-52-832-1151, Fax: +81-52-834-8090

c)

Number of text pages: 28

Number of tables: 3

Number of figures: 8

Number of references: 50

Number of words in Abstract: 249

Number of words in Introduction: 490

Number of words in Discussion: 1190

d) Nonstandard abbreviations

APAP, acetaminophen; CAR, constitutive androstane receptor; CYP, cytochrome P450; DME, drug-metabolizing enzyme; NAC, *N*-acetyl-L-cysteine; Nrf2, NF-E2-related factor-2; PCR, polymerase chain reaction; PB, phenobarbital; TBARS, thiobarbituric acid reactive substances; UGT, UDP-glucuronosyltransferase

DMD Fast Forward. Published on December 18, 2015 as DOI: 10.1124/dmd.115.067439
This article has not been copyedited and formatted. The final version may differ from this version.

Abstract

UDP-glucuronosyltransferase (UGT), a phase II drug-metabolizing enzyme, is expressed in the brain and can catalyze glucuronidation of endogenous and exogenous substrates in the brain. Thus, changes in UGT1A expression could affect homeostasis and drug efficacy. Phenobarbital (PB), a typical inducer of drug-metabolizing enzymes, has been reported to induce oxidative stress and epigenetic changes, which could alter UGT expression in the brain. Here, we aimed to clarify the effects of PB on Ugt1a6 and Ugt1a7 gene expression in rat brains. Sprague-Dawley rats were treated intraperitoneally with PB (80 mg/kg), once daily for 7 days. Ugt1a6 and Ugt1a7 mRNA expression levels were increased in the striatum and thalamus (Ugt1a6: 3.0- and 2.9-fold, respectively; Ugt1a7: 2.6- and 2.6-fold, respectively). Acetaminophen glucuronidation was also increased in the medulla oblongata and thalamus by 1.8- and 1.2-fold, respectively. The induction rates within different brain regions were correlated with Ugt1a6 and Ugt1a7 mRNA expression, and the degree of induction also correlated with that of Nrf2 mRNA. Measurement of oxidative stress markers suggested that PB induced oxidative stress in brain regions in which Ugt1a6 and Ugt1a7 mRNAs were increased. Moreover, histone modifications were altered by PB treatment, resulting in increased histone H3 lysine 4 trimethylation in the striatum and thalamus and decreased histone H3 lysine 9 trimethylation in the thalamus. These results suggested that oxidative stress and histone modifications may promote transcriptional activation of Ugt1a6 and Ugt1a7 genes. In summary, Ugt1a6 and Ugt1a7 mRNA levels were increased by PB treatment, which may alter pharmacokinetics in the brain.

Introduction

Many drug-metabolizing enzymes (DMEs) are expressed primarily in the liver and play important roles in the metabolism of various exogenous and endogenous compounds. Because some DMEs are also found in extrahepatic tissues, including the brain, local brain metabolism could affect the efficacy of central-acting drugs and endogenous compounds, independent of liver metabolism (Dutheil et al., 2008; Miksys and Tyndale, 2013).

UDP-glucuronosyltransferase (UGT) catalyzes a major phase II reaction and has been reported to be expressed in brain tissues, neurons, and astrocytes (King et al., 1999; Suleman et al., 1998; Shelby et al., 2003). Therefore, UGT1As in the brain would be involved in mediating the pharmacological effects of several central-acting drugs as UGT substrates, such as acetaminophen (APAP) (Court et al., 2001), amitriptyline (Green et al., 1998), and valproic acid (Ethell et al., 1998). UGT1As also catalyze the glucuronidation of neurotransmitters and neurosteroids, such as serotonin (Krishnaswamy et al., 2003), dopamine (Itäaho et al., 2009), and estradiol (Court, 2005), as endogenous substrates in the brain. Thus, changes in the expression levels of UGT1As in the brain may affect drug efficacy and homeostasis.

The expression levels of UGT are regulated by various inducers through nuclear receptors, such as aryl hydrocarbon receptor (Yueh et al., 2005; Münzel et al., 2003), constitutive androstane receptor (CAR) (Sugatani et al., 2005), and NF-E2-related factor-2 (Nrf2) (Shen and Kong, 2009). Phenobarbital (PB), a major antiepileptic drug, is a typical DME inducer functioning through CAR signaling pathway and activation of

DMD Fast Forward. Published on December 18, 2015 as DOI: 10.1124/dmd.115.067439
This article has not been copyedited and formatted. The final version may differ from this version.

target gene transcription. Ugt1a6 mRNA has been reported to be increased by PB in the rat liver (Kato et al., 2005). Moreover, previous studies have revealed that PB induces oxidative stress in the rat liver and brain (Dostalek et al., 2008; Reeta et al., 2011). Oxidative stress can activate the Nrf2 signaling pathway, and Ugt1a6 and Ugt1a7 mRNA levels are increased by oxidative stress in rat astrocytes (Reeta et al., 2011). Since Ugt1a6 is expressed in the rat brain, neurons, and astrocytes (Shelby et al., 2003; Sulman et al., 1998), PB is thought to have the potential to change the expression of Ugt1a6 and Ugt1a7 isoforms in the rat brain.

PB can also alter DNA methylation and histone modifications (Watson and Goodman, 2002; Lempiäinen et al., 2011). Such epigenetic changes are involved in gene regulation prior to transcriptional activation. In a previous study, PB-mediated changes in DNA methylation and histone modification were shown to be associated with the upregulation of cytochrome P450 (Cyp) 2b10 (a CAR target gene) in mice (Lempiäinen et al., 2011). Moreover, CAR activation has been shown to be related to epigenetic changes at the promoter region of CAR target genes (Chen et al., 2012). Thus, Ugt1a6 and Ugt1a7 can be induced by PB and affect drug metabolism and homeostasis in the brain.

The purpose of this study was to ascertain whether changes of UGT1A6 and UGT1A7 occurred in rat brain due to PB. If such changes occurred, we sought to clarify their mediating mechanisms.

DMD Fast Forward. Published on December 18, 2015 as DOI: 10.1124/dmd.115.067439
This article has not been copyedited and formatted. The final version may differ from this version.

Materials and Methods

Materials

Thiobarbituric acid was purchased from Cayman Chemical Company (Ann Arbor, MI). *N*-Acetyl-L-cysteine (NAC), APAP, barbital, PB, and 1,1,3,3-tetramethoxypropan were purchased from Wako Pure Chemicals (Osaka, Japan). APAP glucuronide was obtained from Sigma-Aldrich (St. Louis, MO). All other chemicals and solvents were of the highest grade commercially available.

Animal treatment

The present study was approved by the Institutional Animal Care and Use Committee of Meijo University. Eight-week-old male Sprague-Dawley rats (Japan SLC, Hamamatsu, Japan) were treated intraperitoneally once daily for 7 days with PB at a dose of 80 mg/kg/day or with saline as the control. Twenty-four hours after the last treatment, the cerebellum, frontal cortex, parietal cortex, piriform cortex, hippocampus, medulla oblongata, olfactory bulb, striatum, and thalamus were excised from the brain.

RNA extraction and quantitative real-time polymerase chain reaction (PCR)

Total RNA was extracted using TRIzol reagent (Life Technologies, Carlsbad, CA) and was then treated with DNase I (Promega, Madison, WI). Reverse transcription was conducted with ReverTra Ace qPCR RT Kit (Toyobo, Osaka, Japan). Absolute quantitative real-time PCR was performed using the method described by Leong et al. (2007) with slight modifications. Primers were designed for preparation of UGT standard solution (Table 1) and synthesized by Greiner Bio-one (Tokyo, Japan). Using the average molecular weight of the amplified product and Avogadro's constant, the number of copies

per unit volume was calculated. The standard series and samples were run under the same conditions. PCR was performed using Thermal Cycler Dice instrument from TaKaRa Bio (Shiga, Japan) with SYBR Premix Ex Taq II (TaKaRa Bio). The primers used for quantification of UGT mRNA are described in Table 2 and were commercially synthesized by Greiner Bio-one. The PCR amplification conditions were as follows: initial denaturation at 95°C for 30 s; 40 cycles of denaturation at 95°C for 5 s; and annealing and extension at 60°C for 30 s. Taqman Gene expression assays was used to determine the expression of Cyp2b1 mRNA (Rn01457880_m1; Applied Biosystems, Carlsbad, CA). PCR amplification was performed with the same conditions described above. All data were normalized to the expression level of β-actin. Data are shown as the mean values from five rats in each group.

Preparation of microsomes

Pooled rat brain microsomes were prepared from 10 rats according to the methods described previously (Sakakibara et al., 2015) and stored at -80°C until analysis. Protein concentrations were determined using Bio-Rad Protein Assay kit (Bio-Rad, Hercules, CA).

APAP glucuronidation

APAP glucuronidation was determined using the method described by Sakakibara et al. (2014) with slight modifications. In a preliminary study, we confirmed the linearity of the protein concentrations, substrate concentration, and incubation times. The concentrations of APAP and brain microsomes were 1 mM and 0.5 mg/mL, respectively. The reaction mixture was incubated at 37°C for 60 min. Data are presented as the mean of three

independent determinations using pooled brain microsomes from 10 rats.

Immunoblot analysis

The pooled cytoplasmic and nuclear extracts of the striatum and thalamus from rat brains and livers were prepared using NE-PER Nuclear and Cytoplasmic Extraction Reagents (Thermo Fisher Scientific, Waltham, MA) according to the manufacturer's instructions. The cytoplasmic and nuclear extracts were collected and stored at -80°C until SDS polyacrylamide gel electrophoresis and immunoblotting. Immunodetection was performed with a polyclonal rabbit anti-CAR antibody (ab35850; abcam, Cambridge, MA) at a 1:1000 dilution. Immunodetection for glyceraldehyde-3-phosphate dehydrogenase (GAPDH) and Lamin B1 was carried out using anti-GAPDH antibody (ab8245; abcam; 1:500 dilution) and anti-Lamin B1 antibody (ab16048; abcam; 1:5000 dilution), respectively. The bands were scanned using ImageQuant LAS-4010 instrument and quantitated with ImageQuant TL (GE Healthcare Life Science, Uppsala, Sweden).

Thiobarbituric acid reactive substances (TBARS) measurement

For determination of TBARS levels, brain tissues from five rats were pooled and homogenized in 10 volumes (w/v) of 1.15% KCl. TBARS was measured according to the method described by Ohkawa et al. (1979). TBARS were calculated as nmol of TBARS per mg of protein.

Glutathione assay

For determination of the glutathione levels, brain tissues from five rats were pooled and homogenized in 5% sulfosalicylic acid in an ice-water bath. Homogenates consisting of 100 mg tissue in 1 mL (10%) were centrifuged at 8,000 g for 10 min at 4°C to remove

DMD Fast Forward. Published on December 18, 2015 as DOI: 10.1124/dmd.115.067439
This article has not been copyedited and formatted. The final version may differ from this version.

proteins. Supernatants were assayed for glutathione using GSSG/GSH Quantification Kit (Dojindo, Kumamoto, Japan) according to the manufacturer's instructions.

Effects of PB and NAC treatment on Ugt1a6, Ugt1a7 and Cyp2b1 expression in rat hepatocytes

Hepatocytes were isolated from 5-week-old male Sprague-Dawley rats (n = 5) using a two-step collagenase perfusion method. Drug treatments were initiated 24 h after plating. Hepatocytes were treated with 2 mM PB and/or 10 mM NAC for 72 h and were collected for RNA preparation.

DNA methylation assay

Genomic DNA from pooled rat brains (n = 5) was extracted with phenol/chloroform followed by ethanol precipitation (Brilliant et al., 1991) and was assayed for methylated DNA using Methylated DNA Quantification kit (abcam) according to the manufacturer's instructions.

Histone modification assay

Histone extracts from pooled rat brains (n = 5) were prepared using EpiSeeker Histone Extraction Kit (abcam). The histone extracts were assayed for histone modification using Histone H3 (tri-methyl K4), Histone H3 (tri-methyl K9), and Histone H3 (acetyl K9) Quantification Kits (abcam) according to the manufacturer's instructions.

Quantification of PB concentrations

The concentrations of PB in plasma and brain tissues were measured by high-performance liquid chromatography with tandem mass spectrometry. Brain tissue was homogenized in 10 volumes (w/v) of the homogenate buffer containing 10 mM

DMD Fast Forward. Published on December 18, 2015 as DOI: 10.1124/dmd.115.067439
This article has not been copyedited and formatted. The final version may differ from this version.

Tris-HCl, 0.1 mM EDTA, and 20% glycerin. Fifty microliters of brain homogenate or plasma and 200 μL of acetonitrile containing 0.25 μg/mL barbital as internal standard were mixed. The acetonitrile mixtures were vortexed and then centrifuged at 9,000 g for 10 min. Ten microliters of the obtained supernatant was subjected to high-performance liquid chromatography with tandem mass spectrometry. Liquid chromatography was performed using a Prominence instrument, which was equipped with an Inertsil ODS-3 column (3.0 × 150 mm). The column temperature was 40˚C, and the flow rate was 0.2 mL/min. The mobile phase consisted of acetonitrile/10 mM ammonium acetate (40:60 [v/v]). The liquid chromatographic column was connected to an API4000 tandem mass spectrometer operated in the negative electrospray ionization mode. The turbo gas was maintained at a temperature of 300˚C. Mass/charge (*m/z*) ion transitions were recorded in the multiple reaction-monitoring mode, with *m/z* 231.0/187.8 for PB and *m/z* 182.7/139.8 for barbital. The limit of detection for PB was 1.7 pmol with a coefficient of variation of less than 10%. Data are shown as the mean values for five rats in each group.

Statistical analysis

Statistical analyses were performed using Student's paired t-tests with the Kaleida-Graph computer program (Synergy Software, Reading, PA).

Results

Effects of PB on Ugt1a6 and Ugt1a7 mRNA expression in rat brains

Constitutive expression of Ugt1a6 and Ugt1a7 mRNAs was observed in all nine regions, and the expression levels were 1.5–10% of the expression levels in the liver.

DMD Fast Forward. Published on December 18, 2015 as DOI: 10.1124/dmd.115.067439
This article has not been copyedited and formatted. The final version may differ from this version.

Following treatment with PB, Ugt1a6 and Ugt1a7 mRNA levels were increased in the piriform cortex, hippocampus, medulla oblongata, olfactory bulb, striatum, and thalamus; the degree of induction differed among the nine regions examined in this study (Fig. 1). Ugt1a6 and Ugt1a7 mRNA levels were particularly increased in the striatum and thalamus (Ugt1a6: 3.0- and 2.9-fold, respectively; Ugt1a7: 2.6- and 2.6-fold, respectively). The degrees of induction of Ugt1a6 and Ugt1a7 were correlated ($r = 0.92$, $p < 0.001$).

Effects of PB on APAP glucuronidation in rat brains

APAP glucuronidation, which is catalyzed mainly by Ugt1a6 and Ugt1a7, was determined in the medulla oblongata, striatum, and thalamus, where relatively high mRNA induction was observed. Following PB treatment, APAP glucuronidation increased in the medulla oblongata by 1.8-fold (control: 0.23 ± 0.01 pmol/min/mg protein, PB: 0.41 ± 0.01 pmol/min/mg protein). In the thalamus, APAP glucuronidation also increased by 1.2-fold (control: 0.19 ± 0.01 pmol/min/mg protein, PB: 0.23 ± 0.00 pmol/min/mg protein). However, APAP glucuronidation remained unchanged in the striatum (control: 0.23 ± 0.01 pmol/min/mg protein, PB: 0.22 ± 0.01 pmol/min/mg protein).

Effects of PB on the expression levels of nuclear receptors in rat brains

The constitutive expression levels of CAR and Nrf2 mRNAs were detected in all nine regions of the brain, with different degrees of expression (Figs. 2 and 4A). Following treatment with PB, CAR mRNA was not changed in any of the brain regions, with the exception of the medulla oblongata (Fig. 2). Although the expression of the nuclear CAR

DMD Fast Forward. Published on December 18, 2015 as DOI: 10.1124/dmd.115.067439
This article has not been copyedited and formatted. The final version may differ from this version.

protein was increased by 1.5-fold in the liver, it was not increased in the striatum or thalamus, where Ugt1a6 and Ugt1a7 mRNA levels were increased by PB (Fig. 3).

Following PB treatment, Nrf2 mRNA was increased in the hippocampus, medulla oblongata, olfactory bulb, striatum, and thalamus by 1.3-, 1.3-, 1.6-, 2.4-, and 2.0-fold, respectively (Fig. 4A). The degree of induction of Nrf2 mRNA by PB was correlated with that of Ugt1a6 and Ugt1a7 mRNAs (Ugt1a6: $r = 0.97$, $p < 0.001$; Ugt1a7: $r = 0.90$, $p < 0.001$) (Fig. 4B).

Effects of PB on oxidative stress markers in rat brains

The level of TBARS (lipid peroxidation) and total glutathione (nonenzymatic antioxidant defenses) were significantly increased in the medulla oblongata, olfactory bulb, striatum, and thalamus after PB treatment (Figs. 5A and 5B). HO-1 mRNA (regulated by Nrf2) was increased in all nine regions (Fig. 6), and the fold changes of HO-1 mRNA correlated with those of Ugt1a6 and Ugt1a7 mRNA (Ugt1a6: $r = 0.84$, $p < 0.01$; Ugt1a7: $r = 0.89$, $p < 0.01$).

Effects of NAC on Ugt1a6, Ugt1a7 and Cyp2b1 mRNA expression in rat hepatocytes treated with PB

Following PB exposure for 72 h, Ugt1a6 and Ugt1a7 mRNAs were increased by 1.9- and 1.7-fold, respectively, in rat hepatocytes (Fig. 7). NAC treatment decreased the induction of Ugt1a6 and Ugt1a7 mRNAs by 1.1- and 1.2-fold, respectively. PB treatment also increased HO-1 mRNA by 3.0-fold; this effect was inhibited by NAC. Cyp2b1, a representative target gene of CAR, was induced by PB, and unlike Ugt1a6 and Ugt1a7, the level of induction was not decreased by NAC treatment (Fig. 7).

DMD Fast Forward. Published on December 18, 2015 as DOI: 10.1124/dmd.115.067439
This article has not been copyedited and formatted. The final version may differ from this version.

Effects of PB on DNA methylation and histone modifications in rat brains

Following treatment with PB, DNA methylation was unchanged in five brain regions (Fig. 8A). Histone H3 lysine 4 (H3K4) trimethylation was increased by 2.7- and 2.9-fold in the striatum and thalamus, respectively (Fig. 8B), whereas histone H3 lysine 9 (H3K9) trimethylation was decreased by 0.34-fold in the thalamus (Fig. 8C). H3K9 acetylation was unchanged in the five regions (Fig. 8D).

Concentrations of PB in rat brains

The PB concentrations in the brain and plasma were quantified at 1 and 24 h after the last treatment. There were no significant differences in PB concentrations in any brain region at 1 and 24 h (Table 3).

Discussion

In the present study, we found that the expression levels of Ugt1a6 and Ugt1a7 mRNAs in the rat brain were increased by PB. The degree of induction differed among the nine examined brain regions, and those of Ugt1a6 and Ugt1a7 mRNAs were correlated. Therefore, the increases in Ugt1a6 and Ugt1a7 mRNA levels can be attributed to similar mechanisms.

PB is a typical inducer promoting the nuclear translocation of CAR, which is normally sequestered in the cytoplasm by the cytoplasmic CAR retention protein (Kobayashi et al., 2003). CAR translocates to the nucleus and heterodimerizes with the retinoid X receptor (RXR) α. The heterodimer then binds to a PB-responsive enhancer module in the region upstream of the promoter in CAR target genes, such as CYP2B, resulting in

DMD Fast Forward. Published on December 18, 2015 as DOI: 10.1124/dmd.115.067439
This article has not been copyedited and formatted. The final version may differ from this version.

transcriptional activation (Honkakoski et al., 1998). In the present study, the expression of the nuclear CAR protein was increased in the liver following PB treatment, whereas the accumulation of CAR protein in the nucleus was not observed in the striatum and thalamus, where the expression levels of Ugt1a6 and Ugt1a7 mRNAs were increased (Fig. 3). In some brain regions, such as the cortex, hippocampus, striatum, and thalamus, PB and 2,4,6-tryphenuldioxane did not affect CYP2B expression; in contrast, these agents caused a dramatic increase in CYP2B expression in the liver (Upandhya et al., 2002; Pustylnyak et al., 2009; Stamou et al., 2014). These results suggested that another mechanism, not involving CAR, may have contributed to the transcriptional activation of Ugt1a6 and Ugt1a7 in the rat brain.

Nrf2 is activated by oxidative/electrophilic stress and translocates to the nucleus from the cytosol, where it binds to the antioxidant response element with the small Maf protein and leads to transcriptional activation of target genes (Shen and Kong, 2009). Because there is an antioxidant response element in the region upstream of Nrf2 gene, Nrf2 is self-regulated in mice (Miao et al., 2005). Ugt1a6 and Ugt1a7 mRNAs are also increased through transcriptional activation by Nrf2 in mice and rats (Buckley and Klaassen, 2009; Shelby and Klaassen, 2006). In this study, we showed that Nrf2 mRNA was increased by PB and that the degree of induction was correlated with those of Ugt1a6 and Ugt1a7 mRNAs (Fig. 4B). Therefore, Ugt1a6 and Ugt1a7 mRNAs were regulated through the Nrf2 signaling pathway. In fact, the level of TBARS was increased in the brain regions where Ugt1a6 and Ugt1a7 mRNAs were increased following the PB treatment (Fig. 5A). These results suggested that oxidative stress was induced by PB in the rat brain,

DMD Fast Forward. Published on December 18, 2015 as DOI: 10.1124/dmd.115.067439
This article has not been copyedited and formatted. The final version may differ from this version.

consistent with a previous study in rats (Reeta et al., 2011). The brain may be more susceptible to oxidative stress because it contains high levels of unsaturated fatty acids, which are the main targets of free radicals and cellular lipid peroxides. Measurement of TBARS is meaningful as an oxidative stress marker in the brain. Moreover, the level of total glutathione was also increased in some brain regions (Fig. 5B). Such increases in glutathione levels could result from the increase in γ-glutamylcysteine synthetase, which catalyzes the rate-limiting step in the *de novo* synthesis pathway of glutathione. The expression of γ-glutamylcysteine synthetase and the level of glutathione in rat neurons and glia cells are increased by oxidative stress through the Nrf2 signaling pathway (Iwata-Ichikawa et al., 1999; Shih et al., 2003). Because the degree of induction of Ugt1a6 and Ugt1a7 mRNAs was correlated with the degree of induction of Nrf2-target gene HO-1, the oxidative stress induced by PB m ay activate Nrf2 signaling pathway. To verify this hypothesis, we examined the effects of the antioxidant NAC on the induction of Ugt1a6 and Ugt1a7 mRNAs by PB in rat hepatocytes. Our data showed that NAC exposure inhibited the induction of Ugt1a6, Ugt1a7, and HO-1 mRNAs but not Cyp2b1 mRNA (Fig. 7). These results indicated that Ugt1a6 and Ugt1a7 mRNAs were increased by oxidative stress derived from PB.

H3K4 trimethylation correlates with activation of gene expression, whereas H3K9 trimethylation is associated with gene silencing (Kimura, 2013). Moreover, H3K4 trimethylation is increased by oxidative stress (Niu et al, 2015). In the present study, H3K4 trimethylation was increased in the striatum and thalamus, and H3K9 trimethylation was decreased in the thalamus. Moreover, the degree of induction of

DMD Fast Forward. Published on December 18, 2015 as DOI: 10.1124/dmd.115.067439
This article has not been copyedited and formatted. The final version may differ from this version.

Ugt1a6 and Ugt1a7 mRNAs by PB in the striatum and thalamus was higher than those in other regions. These results suggested that the regional differences in the degree of the induction in Ugt1a6 and Ugt1a7 may be associated with differences in epigenetic changes induced by PB in the rat brain.

From the above results, we hypothesized that oxidative stress generated by PB and histone modifications may be involved in the transcriptional activation of Ugt1a6 and Ugt1a7; however, the degrees of induction were not associated with the concentrations of PB in each of the nine brain regions (Table 3). A capacities and responses to oxidative stress among the nine brain regions may be varied, which would be expected to cause differences in the transcriptional activation of Ugt1a6 and Ugt1a7 among the nine brain regions.

In the present study, PB increased not only Ugt1a6 and Ugt1a7 mRNAs but also APAP glucuronidation in brain regions with relatively high induction of mRNA. Ugt1a6 and Ugt1a7 are mainly involved in the conjugation of planar phenols, including endogenous compounds (e.g., serotonin) and drugs such as APAP, as well as metabolites of carcinogens, such as benzo(*a*)pyrene-3,6-diphenol (Bock and Köhle 2005). Therefore, Ugt1a6 and Ugt1a7 in the brain may play important roles in detoxification and homeostasis to protect the brain. In the present study, APAP glucuronidation was increased by PB in the medulla oblongata and thalamus where serotonin, a Ugt1a6 substrate, was found (Iceman et al., 2013; Chung et al., 2015). Thus, the concentrations of UGT substrates, including serotonin, may change locally, thereby altering efficacy. However, the increase in APAP glucuronidation was not correlated with the increase in

Ugt1a6 and Ugt1a7 mRNA expression levels in the striatum. A previous report showed that human UGT1A mRNA and protein levels did not always correlate with each other (Izukawa et al., 2009; Ohtsuki et al., 2012; Oda et al., 2012), suggesting that the level of induction of Ugt mRNA does not correlate with the induction of glucuronidation activities. To determine changes in Ugt1a6 and Ugt1a7 enzyme activities in detail may require more specific Ugt1a6 and Ugt1a7 substrates. Similar to previous reports, our data suggested that an unexplained epigenetic mechanism may be involved in the post-transcriptional regulation of Ugt1a6 and Ugt1a7 in the rat brain.

UGTs play important roles in the detoxification of xenobiotics, including drugs and environmental substances, protecting the organism from the effects of hazardous compound. UGTs also function as antioxidants based upon their role in maintaining the redox balance (Kalthoff et al., 2010). Compared with other organs, the brain appears especially susceptible to excessive oxidative stress (Dringen et al., 2000; Bergamini et al., 2004). Hence, the transcriptional activation of UGT isoforms in the brain contributes to the protection of the brain against cytotoxicity.

In summary, in this study, we found that PB induced the expression of Ugt1a6 and Ugt1a7 in rat brains. These changes could affect pharmacological and physiological functions owing to alterations in the concentrations of the drugs in the brain.

Authorship contributions

Participation in research design: Sakakibara, Katoh, and Nadai

Conducted experiments: Sakakibara, Katoh and Kondo

DMD Fast Forward. Published on December 18, 2015 as DOI: 10.1124/dmd.115.067439
This article has not been copyedited and formatted. The final version may differ from this version.

Wrote or contributed to the writing of the manuscript: Sakakibara, Katoh, and Nadai

Reference

Bergamininn CM, Gambetti S, Dondi A, and Cervellati C (2004) Oxygen, reactive oxygen species and tissue damage. *Curr Pharm Des* **10:** 1611-1626.

Bock KW and Köhle C (2005) UDP-glucuronosyltransferase 1A6: structural, functional, and regulatory aspects. *Methods Enzymol* **400:** 57-75. Review.

Brilliant MH, Gondo Y, and Eicher EM (1991) Direct molecular identification of the mouse pink-eyed unstable mutation by genome scanning. *Science* **252:** 566-569.

Buckley DB and Klaassen CD (2009) Induction of mouse UDP-glucuronosyltransferase mRNA expression in liver and intestine by activators of aryl-hydrocarbon receptor, constitutive androstane receptor, pregnane X receptor, peroxisome proliferator-activated receptor alpha, and nuclear factor erythroid 2-related factor 2. *Drug Metab Dispos* **7:** 847-856.

Chen WD, Fu X, Dong B, Wang YD, Shiah S, Moore DD, and Huang W (2012) Neonatal activation of the nuclear receptor CAR results in epigenetic memory and permanent change of drug metabolism in mouse liver. *Hepatology* **56:** 1499-1509.

Chung YH, Lee YJ, Lee HS, Chung SJ, Lim CH, Oh KW, Sohn UD, Park ES, and Jeong JH (2015) Extremely low frequency magnetic field modulates the level of neurotransmitters. *Korean J Physiol Pharmacol* **19:** 15-20.

Court MH (2005) Isoform-selective probe substrates for in vitro studies of human UDP-glucuronosyltransferases. *Methods Enzymol* **400:** 104-116.

Court MH, Duan SX, von Moltke LL, Greenblatt DJ, Patten CJ, Miners JO, and Mackenzie PI (2001) Interindividual variability in acetaminophen glucuronidation by

human liver microsomes: identification of relevant acetaminophen UDP-glucuronosyltransferase isoforms. *J Pharmacol Exp Ther* **299:** 998-1006.

Dostalek M, Hardy KD, Milne GL, Morrow JD, Chen C, Gonzalez FJ, Gu J, Ding X, Johnson DA, Johnson JA, Martin MV, and Guengerich FP (2008) Development of oxidative stress by cytochrome P450 induction in rodents is selective for barbiturates and related to loss of pyridine nucleotide-dependent protective systems. *J Biol Chem* **283:** 17147-17157.

Dringen R, Gutterer JM, and Hirrlinger J (2000) Glutathione metabolism in brain metabolic interaction between astrocytes and neurons in the defense against reactive oxygen species. *Eur J Biochem* **267:** 4912-4916.

Dutheil F, Beaune P, and Loriot MA (2008) Xenobiotic metabolizing enzymes in the central nervous system: Contribution of cytochrome P450 enzymes in normal and pathological human brain. *Biochimie* **90:** 426-436.

Ethell BT, Anderson GD, Beaumont K, Rance DJ, and Burchell B (1998) A universal radiochemical high-performance liquid chromatographic assay for the determination of UDP-glucuronosyltransferase activity. *Anal Biochem* **255:** 142-147.

Green MD, King CD, Mojarrabi B, Mackenzie PI, and Tephly TR (1998) Glucuronidation of amines and other xenobiotics catalyzed by expressed human UDP-glucuronosyltransferase 1A3. *Drug Metab Dispos* **26:** 507-512.

Honkakoski P, Zelko I, Sueyoshi T, and Negishi M (1998) The nuclear orphan receptor CAR-retinoid X receptor heterodimer activates the phenobarbital-responsive enhancer module of the CYP2B gene. *Mol Cell Biol* **18:** 5652-5658.

Iceman KE, Richerson GB, and Harris MB (2013) Medullary serotonin neurons are CO2 sensitive in situ. *J Neurophysiol* **110:** 2536-2544.

Itäaho K, Court MH, Uutela P, Kostiainen R, Radominska-Pandya A, and Finel M (2009) Dopamine is a low-affinity and high-specificity substrate for the human UDP-glucuronosyltransferase 1A10. *Drug Metab Dispos* **37:** 768-775.

Iwata-Ichikawa E, Kondo Y, Miyazaki I, Asanuma M, and Ogawa N (1999) Glial cells protect neurons against oxidative stress via transcriptional up-regulation of the glutathione synthesis. *J Neurochem* **72:** 2334-2344.

Izukawa T, Nakajima M, Fujiwara R, Yamanaka H, Fukami T, Takamiya M, Aoki Y, Ikushiro S, Sakaki T, and Yokoi T (2009) Quantitative analysis of UDP-glucuronosyltransferase (UGT) 1A and UGT2B expression levels in human livers. *Drug Metab Dispos* **37:** 1759-1768.

Kalthoff S, Ehmer U, Freiberg N, Manns MP, and Strassburg CP (2010) Interaction between oxidative stress sensor Nrf2 and xenobiotic-activated aryl hydrocarbon receptor in the regulation of the human phase II detoxifying UDP-glucuronosyltransferase 1A10. *J Biol Chem* **285:** 5993-6002.

Kato Y, Suzuki H, Ikushiro S, Yamada S, and Degawa M (2005) Decrease in serum thyroxine level by phenobarbital in rats is not necessarily dependent on increase in bamazepine with curcumin in experimental models of epilepsy in rats. *Pharmacol Biochem Behav* **99:** 399-394.

King CD, Rios GR, Assouline JA, and Tephly TR (1999) Expression of UDP-glucuronosyltransferases (UGTs) 2B7 and 1A6 in the human brain and

identification of 5-hydroxytryptamine as a substrate. *Arch Biochem Biophy* **365:** 156-162.

Kimura H (2013) Histone modifications for human epigenome analysis. *J Hum Genet* **58:** 439-445.

Krishnaswamy S, Duan SX, Von Moltke LL, Greenblatt DJ, and Court MH (2003) Validation of serotonin (5-hydroxtryptamine) as an in vitro substrate probe for human UDP-glucuronosyltransferase (UGT) 1A6. *Drug Metab Dispos* **31:** 133-139.

Kobayashi K, Sueyoshi T, Inoue K, Moore R, and Negishi M (2003) Cytoplasmic accumulation of the nuclear receptor CAR by a tetratricopeptide repeat protein in HepG2 cells. *Mol Pharmacol* **64:** 1069-1075.

Lempiäinen H, Müller A, Brasa S, Teo SS, Roloff TC, Morawiec L, Zamurovic N, Vicart A, Funhoff E, Couttet P, Schübeler D, Grenet O, Marlowe J, Moggs J, and Terranova R (2011) Phenobarbital mediates an epigenetic switch at the constitutive androstane receptor (CAR) target gene Cyp2b10 in the liver of B6C3F1 mice. *PLoS One* doi: 10.1371/journal.pone.0018216.

Leong DT, Gupta A, Bai HF, Wan G, Yoong LF, Too HP, Chew FT, and Hutmacher DW (2007) Absolute quantification of gene expression in biomaterials research using real-time PCR. *Biomaterials* **28:** 203-210.

Miao W, Hu L, Scrivens PJ, and Batist G (2005) Transcriptional regulation of NF-E2 p45-related factor (NRF2) expression by the aryl hydrocarbon receptor-xenobiotic response element signaling pathway: direct cross-talk between phase I and II drug-metabolizing enzymes. *J Biol Chem* **280:** 20340-20348.

Miksys S and Tyndale RF (2013) Cytochrome P450-mediated drug metabolism in the brain. *J Psychiatry Neurosci* **38:** 152-163.

Münzel PA, Schmohl S, Buckler F, Jaehrling J, Raschko FT, Köhle C, and Bock KW (2003) Contribution of the Ah receptor to the phenolic antioxidant-mediated expression of human and rat UDP-glucuronosyltransferase UGT1A6 in Caco-2 and rat hepatoma 5L cells. *Biochem Pharmacol* **66:** 841-847.

Niu Y, DesMarais TL, Tong Z, Yao Y, and Costa M (2015) Oxidative stress alters global histone modification and DNA methylation. *Free Radic Biol* **82:** 22-28.

Oda S, Nakajima M, Hatakeyama M, Fukami T, and Yokoi T (2012) Preparation of a specific monoclonal antibody against human UDP-glucuronosyltransferase (UGT) 1A9 and evaluation of UGT1A9 protein levels in human tissues. *Drug Metab Dispos* **40:** 1620-1627.

Ohkawa H, Ohishi N, and Yagi K (1979) Assay for lipid peroxides in animal tissues by thiobarbituric acid reaction. *Anal Biochem* **95:** 351-358.

Ohtsuki S, Schaefer O, Kawakami H, Inoue T, Liehner S, Saito A, Ishiguro N, Kishimoto W, Ludwig-Schwellinger E, Ebner T, and Terasaki T (2012) Simultaneous absolute protein quantification of transporters, cytochromes P450, and UDP-glucuronosyltransferases as a novel approach for the characterization of individual human liver: comparison with mRNA levels and activities. *Drug Metab Dispos* **40:** 83-92.

Pustylnyak V, Pivovarova E, Slynko N, Gulyaeva L, and Lyakhovich V (2009) Species-specific induction of CYP2B by 2,4,6-tryphenyldioxane-1,3 (TPD). *Life Sci*

85: 815-821.

Reeta KH, Mehla J, Pahuja M, and Gupta YK (2011) Pharmacokinetic and pharmacodynamic interactions of valproate, phenytoin, phenobarbitone and carbamazepine with curcumin in experimental models of epilepsy in rats. *Pharmacol Biochem Behav* **99:** 399-407.

Sakakibara Y, Katoh M, Suzuki M, Kawabe R, Iwase K, and Nadai M (2014) Effect of adrenalectomy on expression and induction of UDP-glucuronosyltransferase 1A6 and 1A7 in rats. *Biol Pharm Bull* **37:** 618-624.

Sakakibara Y, Katoh M, Kawayanagi T, and Nadai M (2015) Species and tissue differences in serotonin glucuronidation. *Xenobiotica* Nov 2**:** 1-7. [Epub ahead of print]

Shelby MK, Cherrington NJ, Vansell NR, and Klaassen CD (2003) Tissue mRNA expression of the rat UDP-glucuronosyltransferase gene family. *Drug Metab Dispos* **31:** 326-333.

Shelby MK and Klaassen CD (2006) Induction of rat UDP-glucuronosyltransferases in liver and duodenum by microsomal enzyme inducers that activate various transcriptional pathways. *Drug Metab Dispos* **34:** 1772-1778.

Shen G and Kong AN (2009) Nrf2 plays an important role in coordinated regulation of Phase II drug metabolism enzymes and Phase III drug transporters. *Biopharm Drug Dispos* **30:** 345-355.

Shih AY, Johnson DA, Wong G, Kraft AD, Jiang L, Erb H, Johnson JA, and Murphy TH (2003) Coordinate regulation of glutathione biosynthesis and release by

Nrf2-expressing glia potently protects neurons from oxidative stress. *J Neurosci* **23:** 3394-3406.

Stamou M, Wu X, Kania-Korwel I, Lehmler HJ, and Lein PJ (2014) Cytochrome p450 mRNA expression in the rodent brain: species-, sex-, and region-dependent differences. *Drug Metab Dispos* **42:** 239-244.

Sugatani J, Nishitani S, Yamakawa K, Yoshinari K, Sueyoshi T, Negishi M, and Miwa M (2005) Transcriptional regulation of human UGT1A1 gene expression: activated glucocorticoid receptor enhances constitutive androstane receptor/pregnane X receptor-mediated UDP-glucuronosyltransferase 1A1 regulation with glucocorticoid receptor-interacting protein 1. *Mol Pharmacol* **67:** 845-855.

Suleman FG, Abid A, Gradinaru D, Daval JL, Magdalou J, and Minn A (1998) Identification of the uridine diphosphate glucuronosyltransferase isoform UGT1A6 in rat brain and in primary cultures of neurons and astrocytes. *Arch Biochem Biophy* **358:** 63-67.

Thulluri S, Wu M, Blough ER, Manne ND, Litchfield AB, and Wang B (2012) Regulation of iron-related molecules in the rat hippocampus: sex- and age-associated differences. *Ann Clin Lab Sci* **42:** 145-151.

Tian H, Ou J, Strom SC, and Venkataramanan R (2005) Activity and expression of various isoforms of uridine diphosphate glucuronosyltransferase are differentially regulated during hepatic regeneration in rats. *Pharm Res* **22:** 2007-2015.

Upadhya SC, Chinta SJ, Pai HV, Boyd MR, and Ravindranath V (2002) Toxicological consequences of differential regulation of cytochrome p450 isoforms in rat brain

regions by phenobarbital. *Arch Biochem Biophys* **399:** 56-65.

Watson RE and Goodman JI (2002) Effects of phenobarbital on DNA methylation in GC-rich regions of hepatic DNA from mice that exhibit different levels of susceptibility to liver tumorigenesis. *Toxicol Sci* **68:** 51-58.

Yoshinari K, Okino N, Sato T, Sugatani J, and Miwa M (2006) Induction of detoxifying enzymes in rodent white adipose tissue by aryl hydrocarbon receptor agonists and antioxidants. *Drug Metab Dispos* **34:** 1081-1089.

Yueh MF, Kawahara M, and Raucy J (2005) Cell-based high-throughput bioassays to assess induction and inhibition of CYP1A enzymes. *Toxicol In Vitro* **19:** 275-287.

Footnotes

This work was supported in part by JSPS KAKENHI [Grant Number 25460200]; and the Hori Sciences and Arts Foundation.

The authors report no conflicts of interest.

Figure Legends

Fig. 1. Changes in Ugt1a6 (A) and Ugt1a7 (B) mRNA expression in response to PB treatment in rat brains.

Each column represents the mean ± SD of three independent determinations. The mRNA expression levels were normalized to the expression of β-actin mRNA. $^{**}p < 0.01$, $^{***}p < 0.01$ compared with the control.

Fig. 2. Expression levels of CAR mRNA in rat brains following PB treatment.

The expression of CAR mRNA was calculated as the value relative to that of the control in the cerebellum. The mRNA expression level was normalized to the expression of β-actin mRNA. Each column represents the mean ± SD of three independent determinations. $^{**}p < 0.01$ compared with the control.

Fig. 3. Expression levels of CAR protein in rat brains and liver following PB treatment.

The expression of CAR protein was calculated as the value relative to that of the corresponding control. The protein expression level was normalized to those of GAPDH and Lamin B1 in the cytosol and nucleus, respectively. Each column represents the mean ± SD of three independent determinations. $^{*}p < 0.05$, $^{**}p < 0.01$ compared with the control.

Fig. 4. Effects of PB on Nrf2 mRNA (A) and correlation analysis between fold inductions of Nrf2 and Ugt1a mRNAs in rat brains (B).

DMD Fast Forward. Published on December 18, 2015 as DOI: 10.1124/dmd.115.067439
This article has not been copyedited and formatted. The final version may differ from this version.

The expression of Nrf2 mRNA was calculated as the value relative to that of the control in the cerebellum. The mRNA expression level was normalized to the expression of β-actin mRNA. Each column represents the mean ± SD of three independent determinations. *$p < 0.05$, **$p < 0.01$, ***$p < 0.001$ compared with the control. The x-axis represents the relative expression of Ugt1a mRNA the y-axis represents the relative expression of Nrf2 mRNA.

Fig. 5. Effects of PB on TBARS (A) and total glutathione (B) in rat brains.

Each column represents the mean ± SD of three independent determinations. *$p < 0.05$, **$p < 0.01$ compared with the controlf

Fig. 6. Effects of PB on HO-1 mRNA in rat brains.

The expression of HO-1 mRNA was calculated as the value relative to that of the control in the cerebellum. The mRNA expression level was normalized to the expression of β-actin mRNA. Each column represents the mean ± SD of three independent determinations. *$p < 0.05$, **$p < 0.01$, ***$p < 0.001$ compared with the control.

Fig. 7. Inhibition of PB-induced increases in Ugt1a6, Ugt1a7, HO-1 and Cyp2b1 mRNAs in rat hepatocytes by NAC.

The mRNA expression was calculated as the value relative to that of the control. The mRNA expression level was normalized to the expression of β-actin mRNA. Each column represents the mean ± SD of three independent determinations. *$p < 0.05$, **$p <$

0.01 compared with the control.

Fig. 8. Effects of PB on DNA methylation and histone modifications in rat brains. Percentages were calculated as the values relative to that of the control in the cerebellum. Each column represents the mean ± SD of three independent determinations. *$p < 0.05$ compared with the control.

Table 1. Primer sequences prepared for the Ugt standard solution

Gene	Accession No.		Sequence
Ugt1a6	NM_057105	Sense	5’-GAGCACCTCAGTGAACGCGGA-3’
		Anti-sense	5’-ACTCTCTTAGAGGAGCCATCAGG-3’
Ugt1a7	NM_130407	Sense	5’-CAAGGAAAGAGTGTGGAACCTT-3’
		Anti-sense	5’-ATTGGGCATCACAGGTCTGGGTA-3’

Table 2. Primer sequences used for quantification

Gene	Accession No.		Sequence	Amplicon size (bp)	Reference
Ugt1a6	NM_057105	Sense	5’-GGGAGAATCCAAATACTACAGGAG-3’	100	Tian et al. (2005)
		Anti-sense	5’-CAGCAAAGTGGTTGTTCCCAAAGG-3’		
Ugt1a7	NM_130407	Sense	5’-CAGACCCCGGTGACTATGACA-3’	73	Tian et al. (2005)
		Anti-sense	5’-CAACGTGAAGTCTGTGCGTAACA-3’		
CAR	NM_022941	Sense	5’-CGGAGTATAAAACAGCGCATACTCA-3’	72	Tian et al. (2005)
		Anti-sense	5’-AAGCAGCGGCATCATAGCA-3’		
Nrf2	AF037350	Sense	5’-CTCCCAGGTTGCCCACATTC-3’	239	Yoshinari et al. (2006)
		Anti-sense	5’-AAGCAGCGGCATCATAGCA-3’		
HO-1	NM_012940	Sense	5’-TGCTCGCATGAACACTCTG-3’	123	Thulluri et al. (2012)
		Anti-sense	5’-TCCTCTGTCAGCAGTGCCT-3’		
β-actin	NM_031144	Sense	5'-CTGGCCTCACTGTCCACCTT-3'	65	Tian et al. (2005)
		Anti-sense	5'-GGGCCGGACTCATCGTACT-3'		

DMD Fast Forward. Published on December 18, 2015 as DOI: 10.1124/dmd.115.067439
This article has not been copyedited and formatted. The final version may differ from this version.

Table 3. Concentrations of PB in the brain and plasma at 1 and 24 h after administration

	PB (μg/mg protein)	
	1 hr	24 hr
Cerebellum	291.1 ± 32.0	9.0 ± 6.3
Frontal cortex	320.1 ± 34.0	9.1 ± 5.5
Piriform cortex	307.2 ± 23.7	9.1 ± 5.5
Parietal cortex	324.2 ± 34.5	8.9 ± 5.2
Hippocampus	311.8 ± 19.4	9.6 ± 6.5
Medulla oblongata	322.5 ± 27.5	9.7 ± 6.2
Olfactory bulb	306.7 ± 30.9	9.1 ± 6.0
Striatum	320.3 ± 35.6	8.9 ± 6.1
Thalamus	325.7 ± 29.9	9.8 ± 6.0
Plasma	76.1 ± 9.5[a]	2.8 ± 1.7[a]

[a]μg/mL

Fig. 1

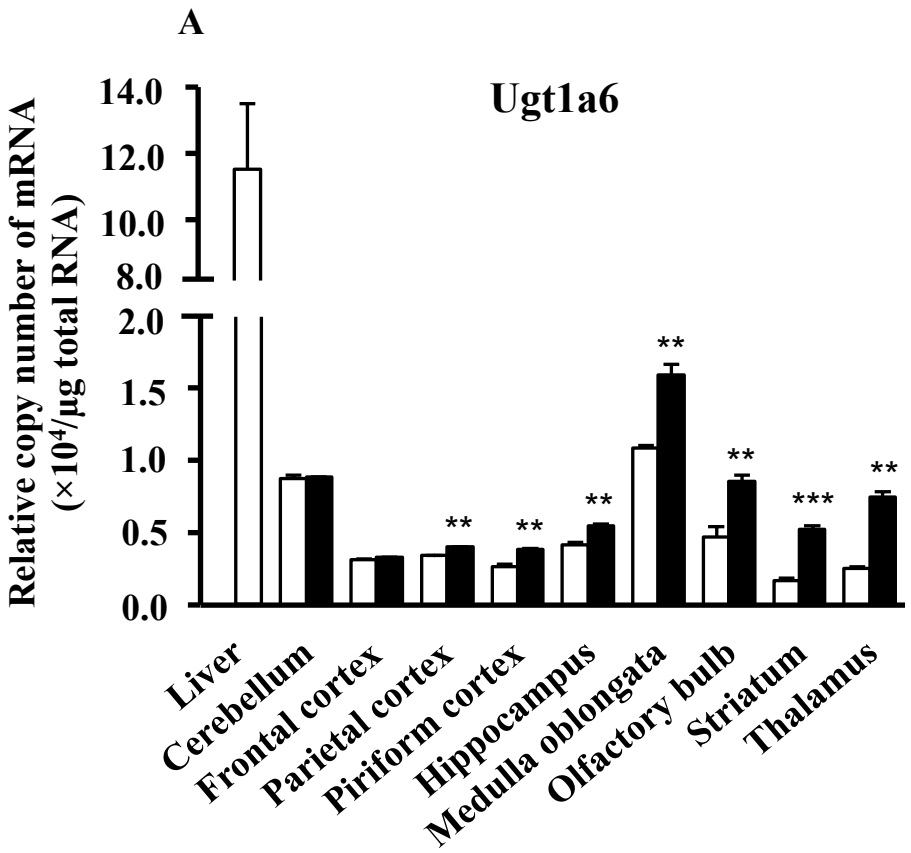

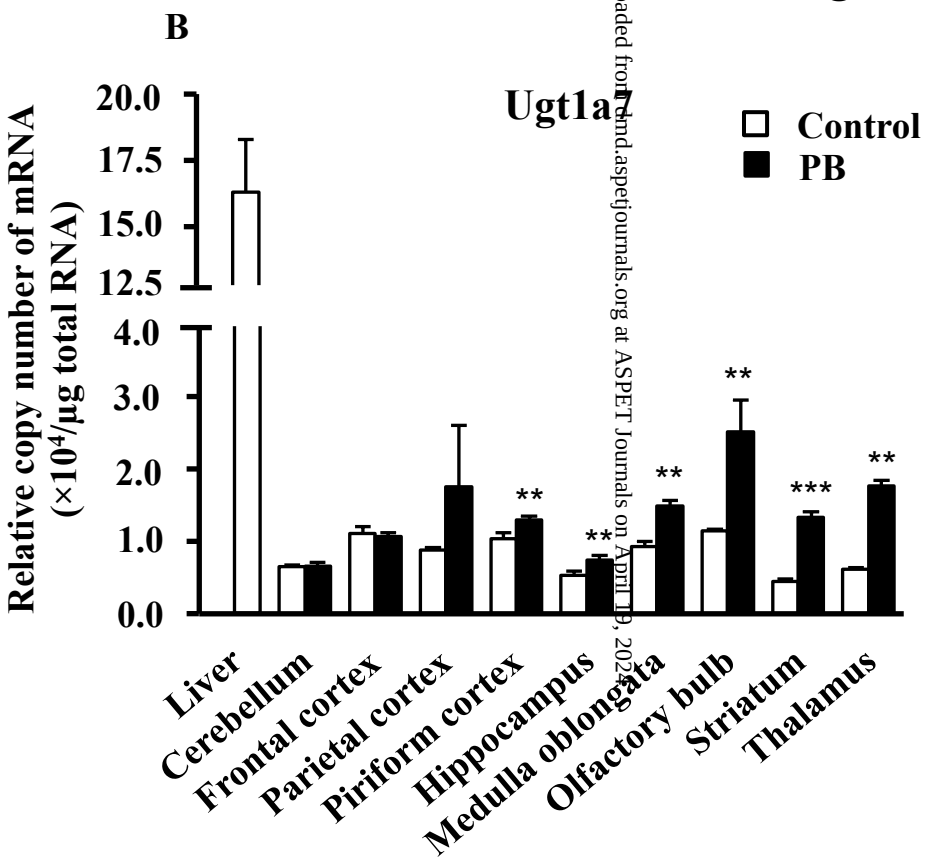

Fig. 2

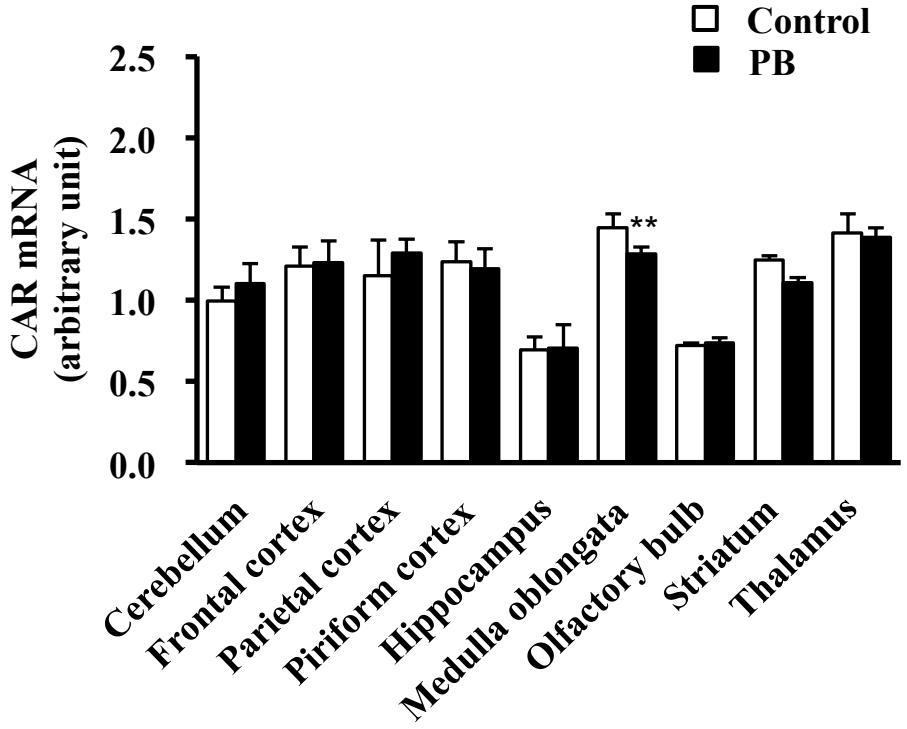

Fig. 3

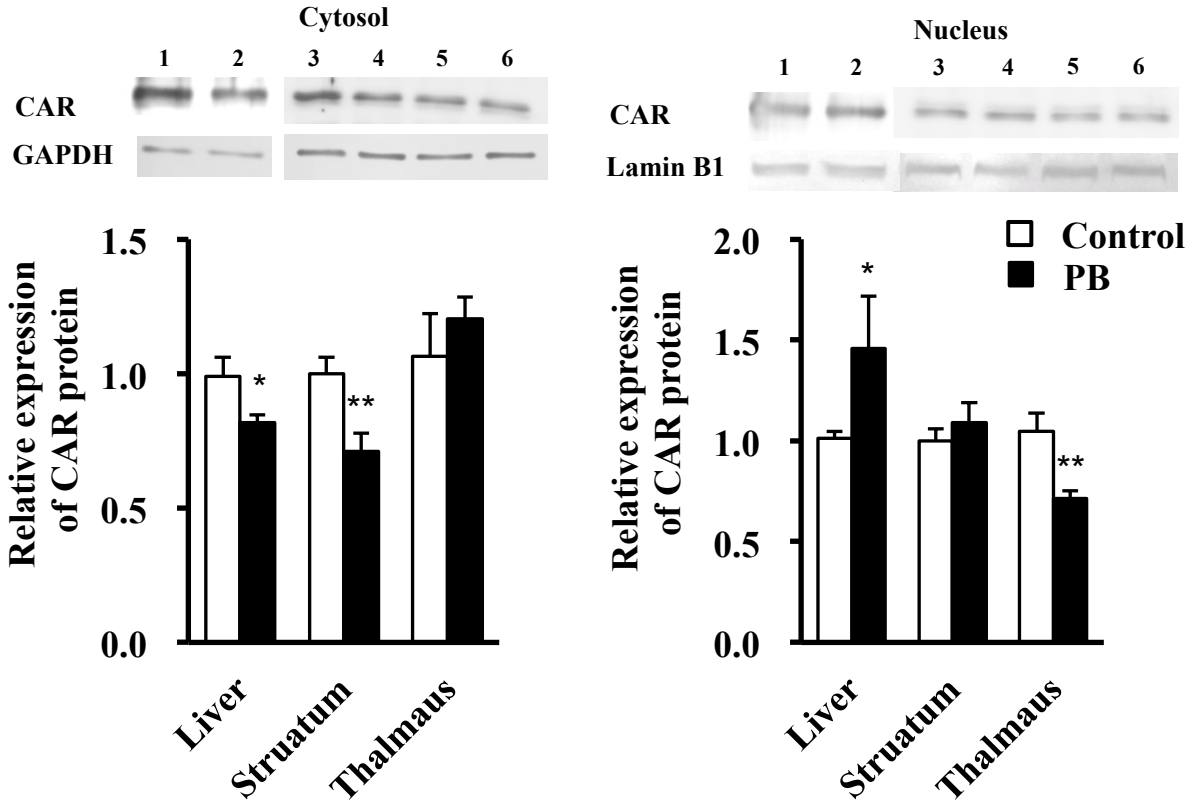

Fig. 4

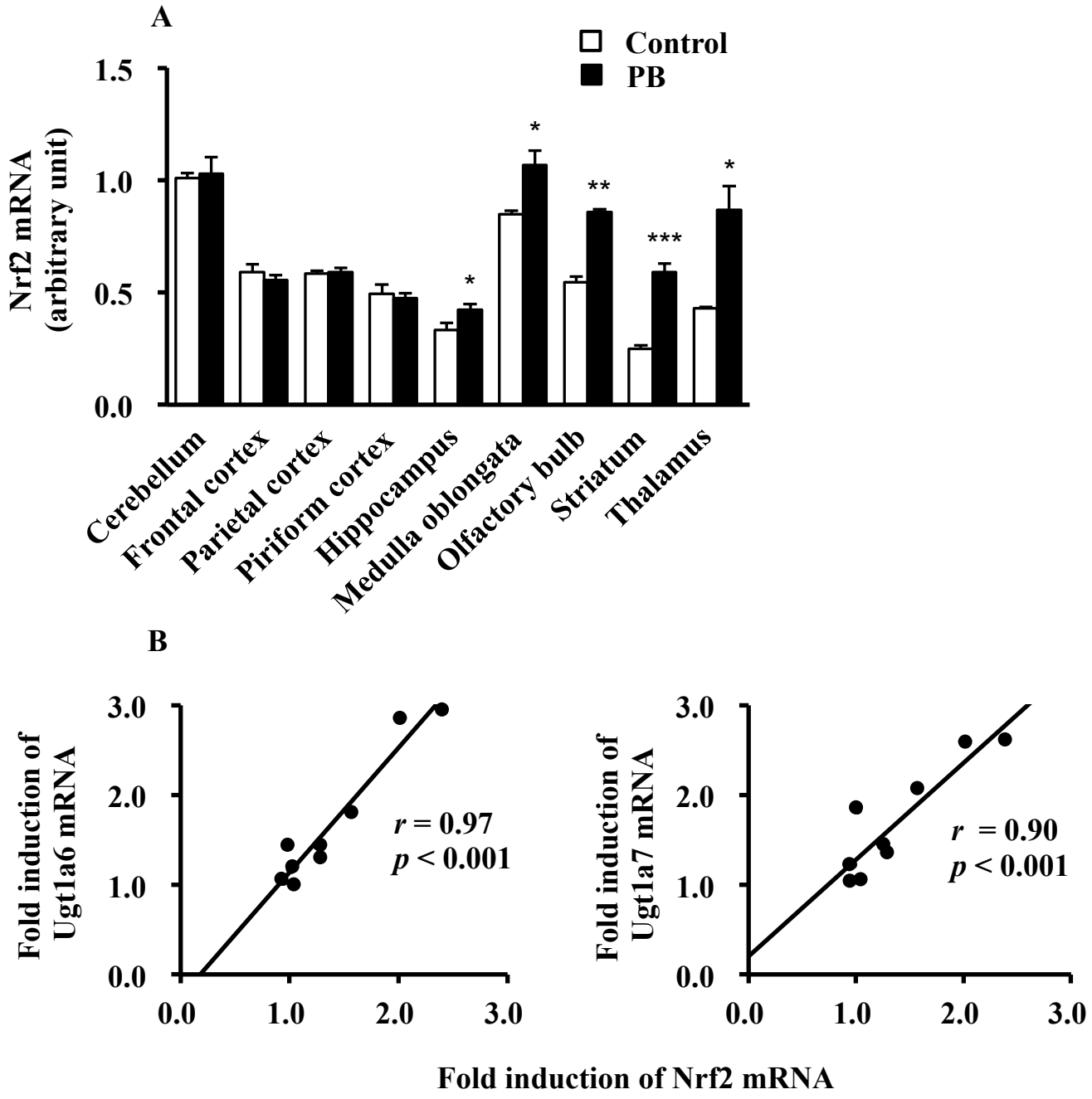

Fig. 5

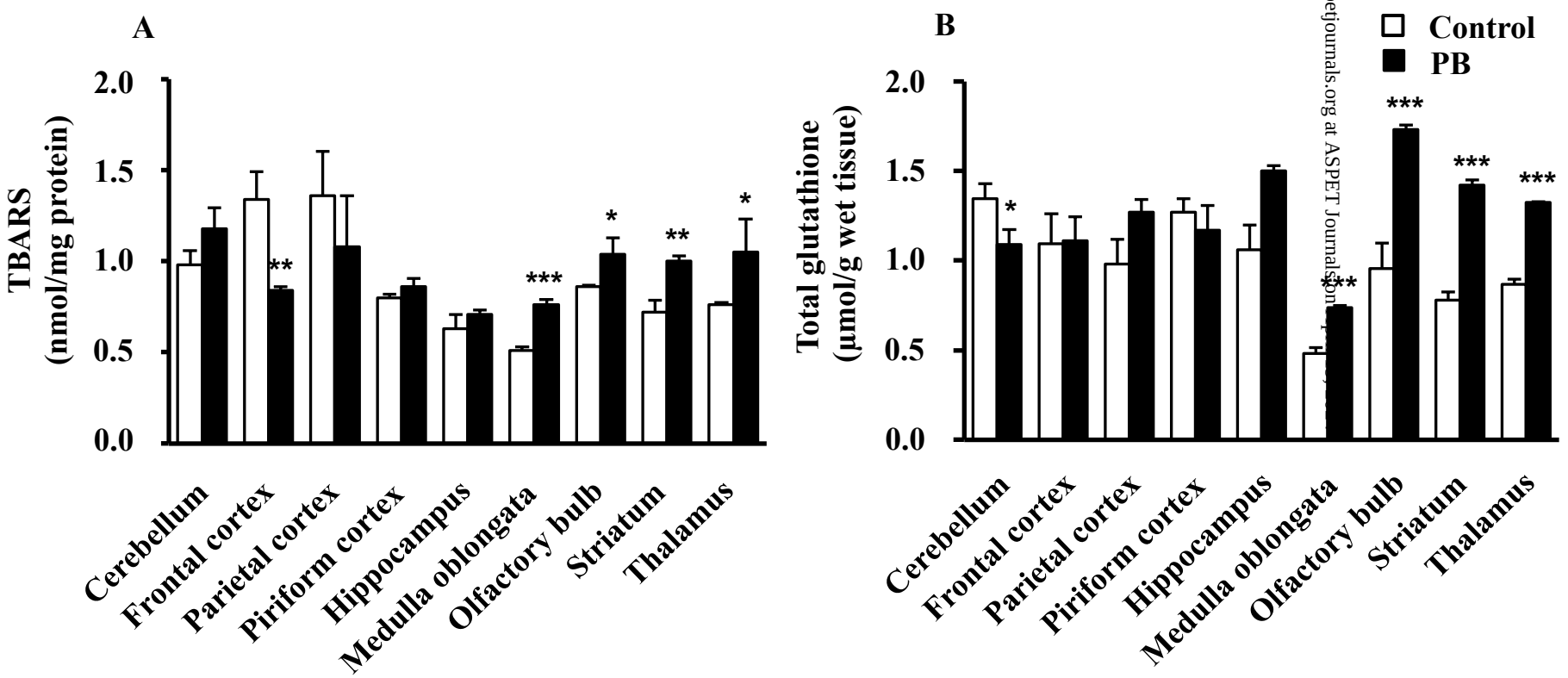

Fig. 6

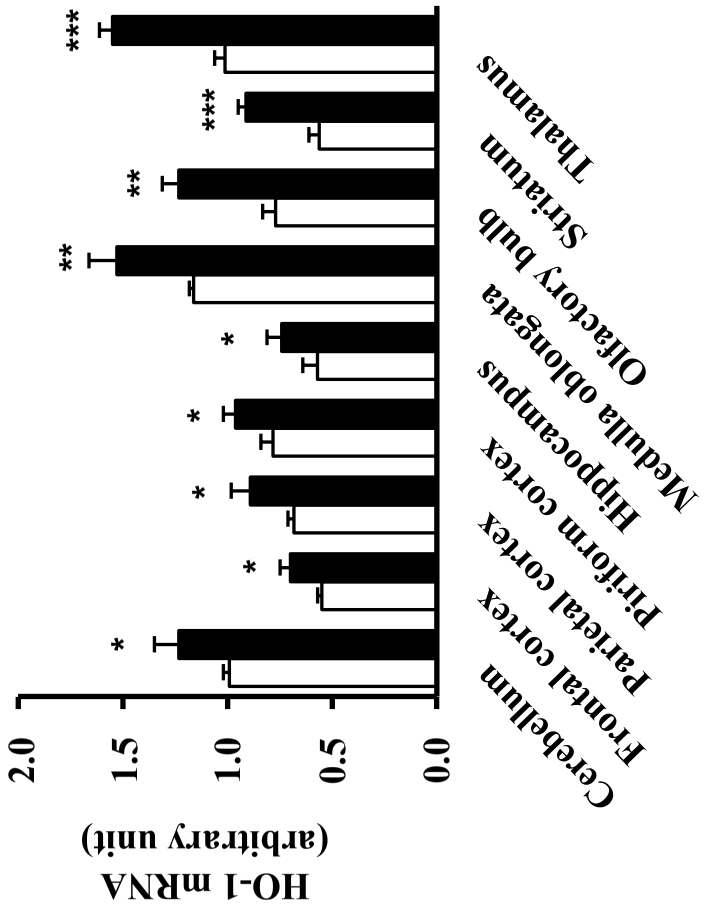

Fig. 7

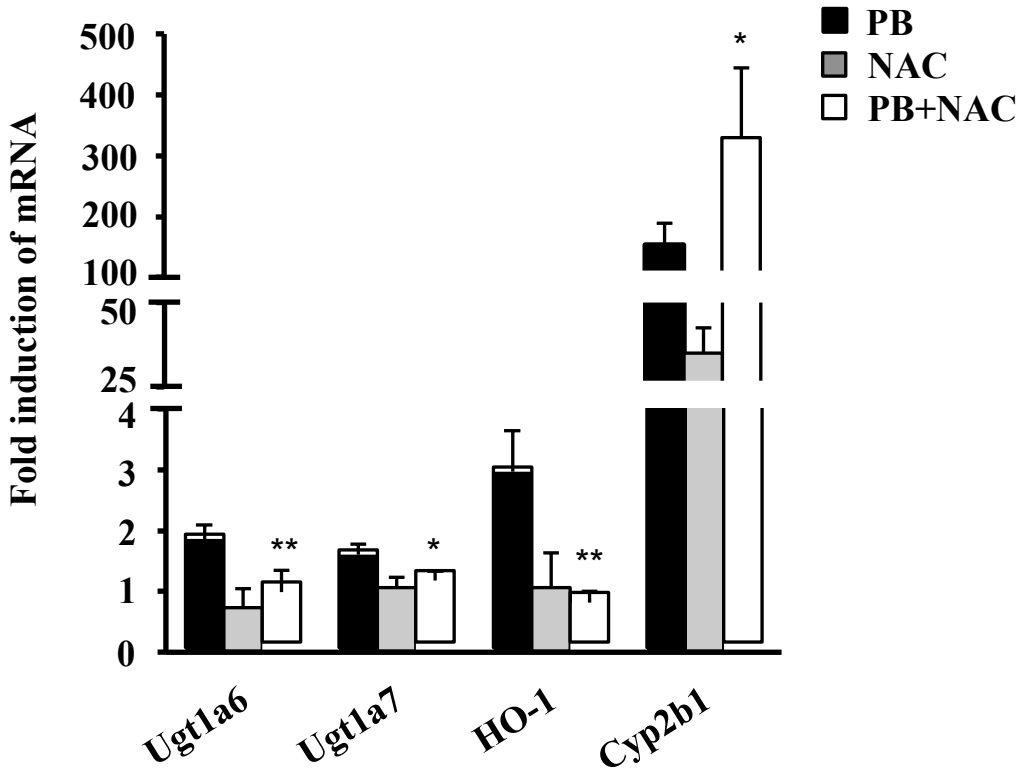

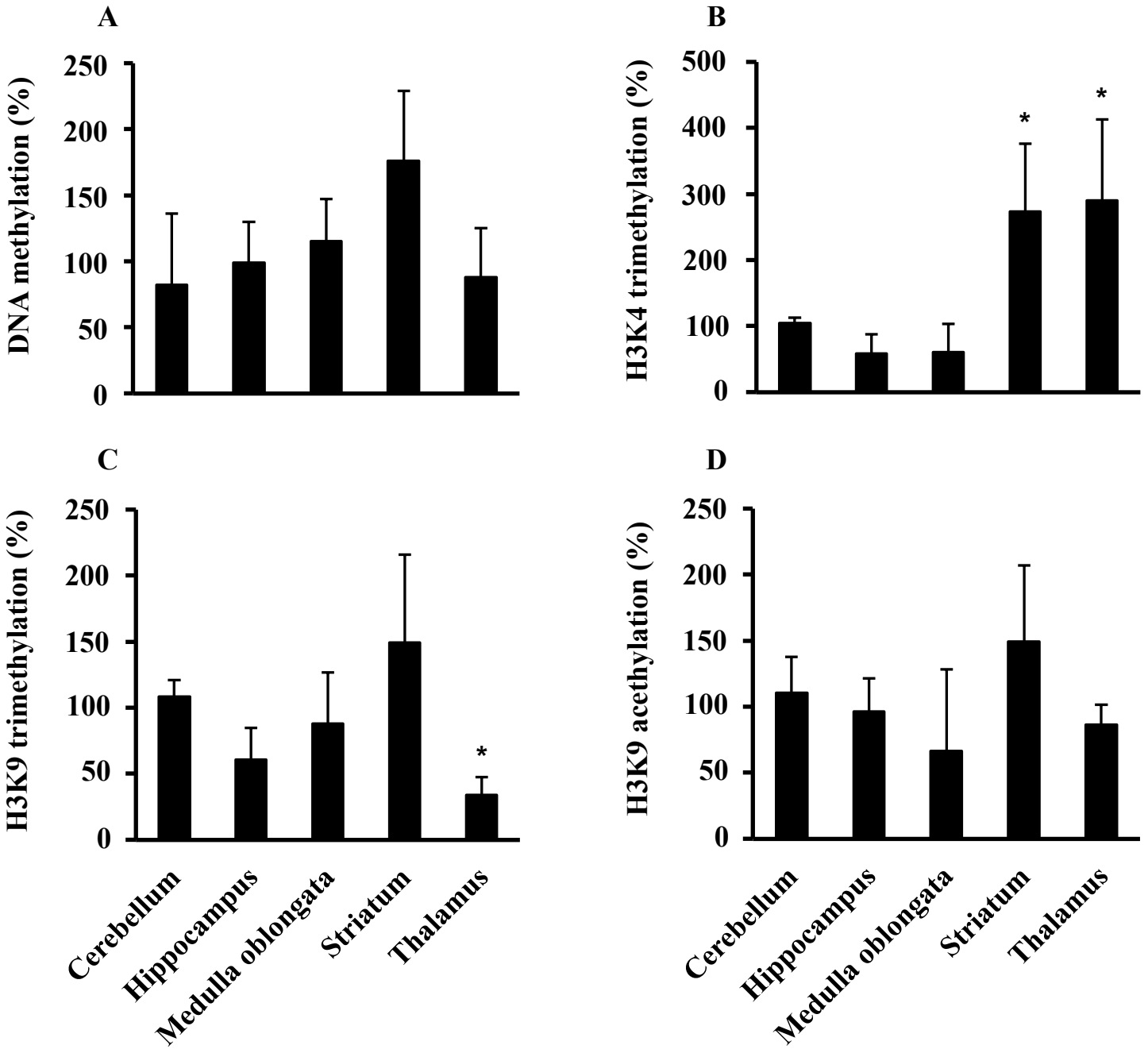

Fig. 8